

Group A

FOIA/PA NO: 2015-0242

## RECORDS BEING RELEASED IN PART

The following types of information are being withheld:

- Ex. 1:  Records properly classified pursuant to Executive Order 13526
- Ex. 2:  Records regarding personnel rules and/or human capital administration
- Ex. 3:  Information about the design, manufacture, or utilization of nuclear weapons  
 Information about the protection or security of reactors and nuclear materials  
 Contractor proposals not incorporated into a final contract with the NRC.  
 Other \_\_\_\_\_
- Ex. 4:  Proprietary information provided by a submitter to the NRC  
 Other \_\_\_\_\_
- Ex. 5:  Draft documents or other pre-decisional deliberative documents (D.P. Privilege)  
 Records prepared by counsel in anticipation of litigation (A.W.P. Privilege)  
 Privileged communications between counsel and a client (A.C. Privilege)  
 Other \_\_\_\_\_
- Ex. 6:  Agency employee PII, including SSN, contact information, birthdates, etc.  
 Third party PII, including names, phone numbers, or other personal information
- Ex. 7(A):  Copies of ongoing investigation case files, exhibits, notes, ROI's, etc.  
 Records that reference or are related to a separate ongoing investigation(s)
- Ex. 7(C):  Special Agent or other law enforcement PII  
 PII of third parties referenced in records compiled for law enforcement purposes
- Ex. 7(D):  Witnesses' and Allegers' PII in law enforcement records  
 Confidential Informant or law enforcement information provided by other entity
- Ex. 7(E):  Law Enforcement Technique/Procedure used for criminal investigations  
 Technique or procedure used for security or prevention of criminal activity
- Ex. 7(F):  Information that could aid a terrorist or compromise security

Other/Comments: \_\_\_\_\_

~~OUO-Security Related Information~~  
~~OFFICIAL USE ONLY~~

Official Use Only/ Circumvention of Statute  
Printed December 2010

**A Comparison of HEMP MHD and Geomagnetic Induced Currents and  
a Preliminary Assessment of Digital System Vulnerability at Nuclear  
Power Plants**

**A Letter Report to the USNRC**

Prepared by:

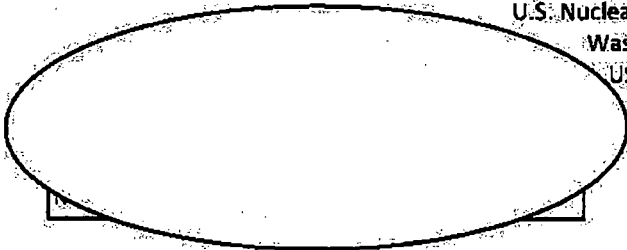
(b)(6)



Sandia National Laboratories  
P.O. Box 5800  
Albuquerque, NM 87185

Prepared for:

Digital Instrumentation & Control Branch  
Office of Nuclear Regulatory Research  
U.S. Nuclear Regulatory Commission  
Washington DC 20555  
USNRC JCN N6432



**Abstract**

A study of the critical digital equipment used at nuclear power plants (NPP) was conducted to determine their susceptibility to potential damage from electromagnetic (EM) signal challenges associated with the magneto-hydrodynamic (MHD) component of a high-altitude EM pulse (HEMP) and with Geomagnetically Induced Currents (GIC) produced by severe space weather events. The goal was to generate an addendum to a 2009 Sandia study on the effects of HEMP and high-power microwaves (HPM) on nuclear power plant safe shutdown systems. The estimated safety margins against HEMP projected signals are deemed sufficient for demonstrating hardness of digital equipment against such threats.

Further dissemination authorized to the Department of Energy and DOE contractors only; other requests shall be approved by the originating facility or higher DOE programmatic authority.

~~OFFICIAL USE ONLY~~

LIMITED INTERNAL

DISTRIBUTION PERMITTED

~~OUO-Security Related Information~~

## 1 Purpose

The goal of this report is to compare deliberate EM threats, discussed in a previous report [Ref. 1], to the threat posed by naturally occurring events; specifically from the electrical insults resulting from geomagnetic storms. The previous report analyzed two types of deliberate threat signals. The first was a directed-energy RF/HPM threat produced by conventional means using pulsed sources and specially designed and tuned antennas. These sources generate a very short, intense energy field often lasting less than a microsecond but having an electric field amplitude that can be on the order of tens of kilovolts per meter. The second was from a high-altitude nuclear electromagnetic pulse (EMP), created when a nuclear weapon is detonated at an altitude of 125-250+ miles above the earth. The nuclear explosion produces a pulse of energy that interacts with the earth's atmosphere below it and nearly simultaneously generates an approximately planar EM wave over the entire continental U.S.

In the previous report, which was itself an update of a similar report completed in 1983 [2], only the Early Time, or E1, portion of the HEMP signal was analyzed (see figure below). This decision was made because it paralleled the analysis approach of the original report and because the E1 field levels and time characteristics were similar to those of the conventional HPM threat values. However, the signals generated by geomagnetic phenomenon can be hundreds of seconds or more in duration and contain field levels on the order of 10 V/km. Because these characteristics more closely resemble the Late Time, or E3, portion of the HEMP threat, the HEMP E1 and E2 signals and the conventional HPM threat signals will not be included in this analysis. For completeness, HEMP E2 signals are considered to be similar in strength and duration to a lightning strike.

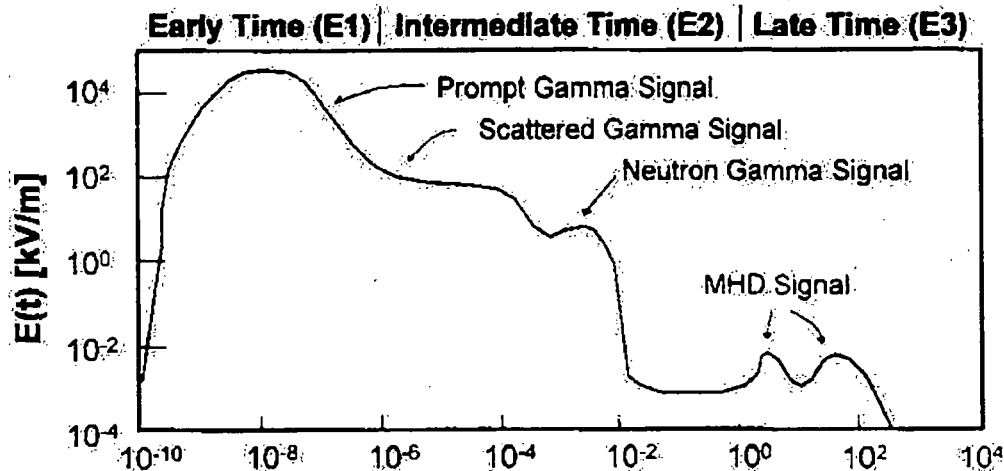


Figure 1: Approximate temporal behavior of HEMP [3]

## 2 THE EM THREATS

### 2.1 The Magneto-Hydrodynamic (MHD) Threat

As mentioned above, an EMP threat signal is created when a nuclear weapon is detonated at an altitude of 125-250+ miles above the earth. The resulting HEMP E1 fields can produce transient voltages on miles of exposed electrical conductors, either above or below ground level, propagating and building to a peak intensity of thousands of volts but with a much longer duration (tens of microseconds). These transient voltage signals can generate large transient currents (hundreds to thousands of amperes) that will be transmitted into facilities through penetration points, propagating through pathways normally used by power generating equipment, computers, communication equipment, etc., until reaching and damaging electronic devices that may be sensitive to such signal-induced stress. This was the primary focus of the previous report.

Additionally, a threat signal is also created by the variation induced in the Earth's magnetic field in response to the nuclear detonation. This late-time EMP energy is also known as the magneto-hydrodynamic (MHD) pulse, or E3 signal. The equation for the electric field arising from the time changing magnetic field at the Earth's surface is given below in Equation 1 [4, p. 3]. This equation is for a single layer model of the Earth with a constant conductivity,  $\sigma$ . Multi-layered models require an additional complex term inside the integral to represent more realistic earth conductivity models. Also, an accurate description of the magnetic field is still required to evaluate this expression.

$$E(t) = \frac{1}{\sqrt{\pi\sigma\mu}} \int_{-\infty}^t \frac{1}{\sqrt{t-t'}} \frac{\partial B(t')}{\partial t'} dt' \quad (1)$$

Using this equation, very complicated coupling calculations would be performed next to determine the currents induced in overhead and buried cables. This is the same approach that was used in the previous report and those equations can be found there. However, most attempts at analysis simplify this process by first considering the underlying physics of the detonation, and the overall shape and magnitude of the resulting waveform.

Physically, there are actually two subcomponents of the E3 signal, the first is called the blast-wave component and the second is the atmospheric heave component. The blast-wave component can be modeled as a quasi-static problem, with a brief, intense magnetic dipole located at the detonation location acting as a perturbation to the overall geomagnetic field. The second component is similar to the first, but it is generated as the heated ionized air from the detonation tries to return to its original state. Both components generate fields of comparable levels, on the order of a few volts per kilometer depending on the conductivity of the ground below, with the first component starting immediately and lasting a few seconds and the second component starting about ten seconds after the detonation and lasting a few hundred seconds, see Figure 2. While it might not seem intuitive, frequency analysis confirms that most of the energy is located below 1Hz, which means in comparison to power systems it is quasi-DC and therefore the threat signal is often treated as a constant. This means that basic DC circuit modeling concepts can be used to perform any further analysis of the problem. Most published research uses simple DC currents on the order of 50A to 200A when testing the effects of MHD on power system components [4, 5].

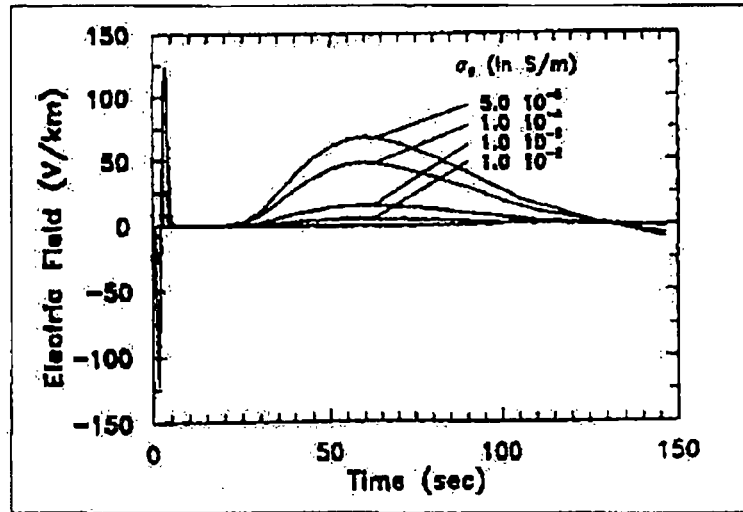


Figure 2: Time Domain Behavior of MHD vs. Conductivity [4]

The HEMP E3 energy footprint on the surface of the Earth, see Figure 3, is distributed differently than the typical "smile" diagram, see Figure 4, described in the previous reports. It is much smaller and forms simple elliptical patterns of varying intensity. Its polarization tends to be orientated more strongly in the east to west direction [184]. Still, it is large enough that a significant DC current will be induced when a long power distribution line is illuminated by an electric field with a strength of only a few tens of volts per kilometer if it is oriented in roughly the same direction.

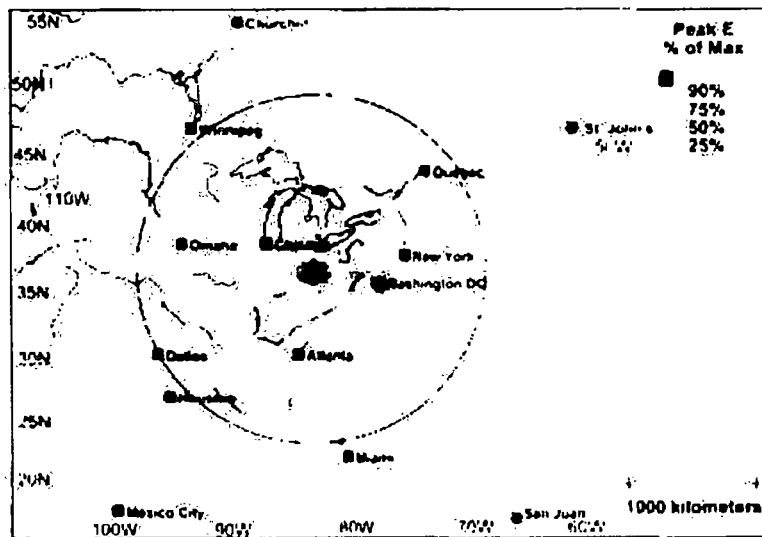


Figure 3: Footprint of Late Time EMP - MHD [6, p. 7]

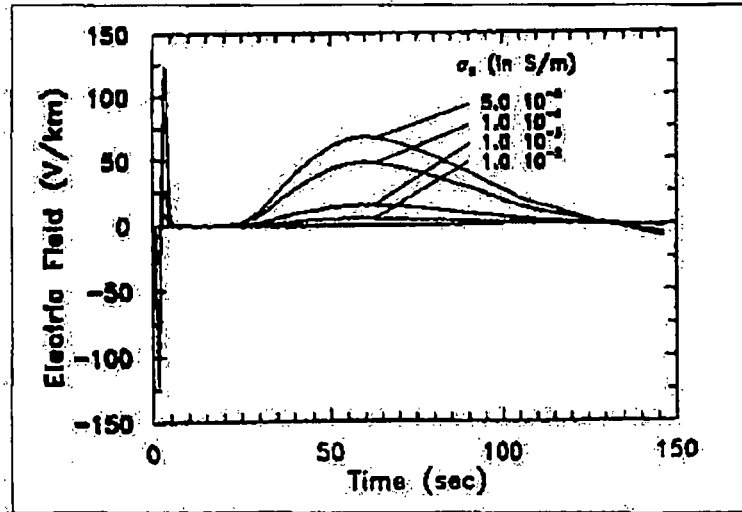


Figure 2: Time Domain Behavior of MHD vs. Conductivity [4]

The HEMP E3 energy footprint on the surface of the Earth, see Figure 3, is distributed differently than the typical "smile" diagram, see Figure 4, described in the previous reports. It is much smaller and forms simple elliptical patterns of varying intensity. Its polarization tends to be orientated more strongly in the east-to-west direction [184]. Still, it is large enough that a significant DC current will be induced when a long power distribution line is illuminated by an electric field with a strength of only a few tens of volts per kilometer if it is oriented in roughly the same direction.

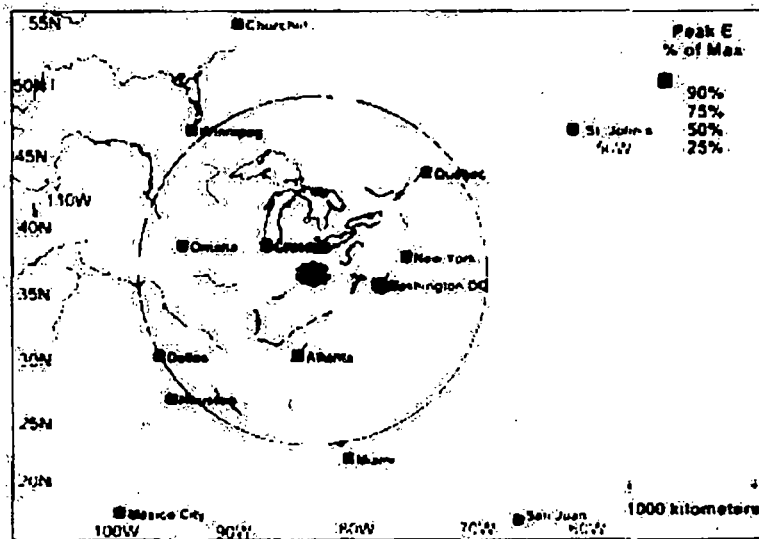


Figure 3: Footprint of Late Time EMP - MHD [6, p. 7]

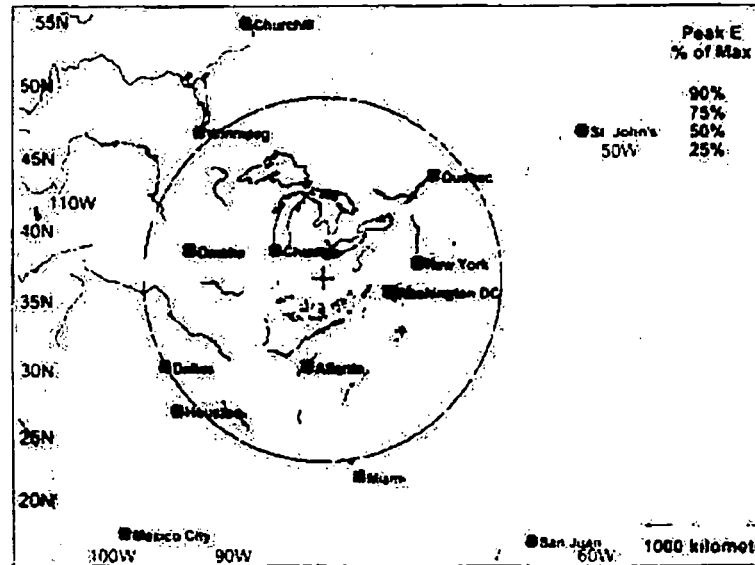


Figure 4: Footprint of Early Time EMP - "Smile Diagram" [6, p. 6]

## 2.2 The Geomagnetic Induced Current (GIC) Threat

### 2.2.1 Space Weather

Geomagnetically Induced Currents (GICs) are the byproduct of an incredibly complex and multistage interaction process between the Earth and the Sun. The process starts at the Sun with its own volatile and variable magnetic field and its production of a steady stream of particles being continuously ejected into space, commonly known as the solar wind. Added to this mixture are the more sporadic solar events, like flares and coronal mass ejections (CMEs), that can throw large, relatively dense clouds of plasma out into interplanetary space as well. CMEs and regions of the solar wind travelling at different speeds interact with each other during their journey away from the Sun, producing countless combinations of solar wind conditions when they finally reach the Earth several days later. These conditions include the speeds, densities and temperatures (kinetic energies) of the solar wind particles as well as the strengths and orientations of its electric and magnetic fields. This overall interplanetary environment that the Earth encounters is often called Space Weather.

Space Weather interacts with the Earth's magnetic field, creating the magnetosphere; a region formed as the Earth's own magnetic field tries to balance itself against the interplanetary environment and forms a protective region around the Earth. The transient and fluctuating nature of Space Weather prevents this protective layer from being completely impenetrable and energized plasma from the solar wind finds several ways to couple into the magnetosphere. The magnetosphere responds by changing and flowing in an attempt to reach a new point of internal equilibrium and external balance. These changes within the magnetosphere are fundamentally nothing more than plasma currents and electromagnetic fields inducing and coupling energy into each other and also into the Earth's ionosphere. The ionosphere is the spherical region around the Earth beneath the magnetosphere where ions and electrons created by solar radiation exist in the largest densities.

~~OUO Security Related Information~~  
~~OFFICIAL USE ONLY~~

The motions of these charged particles generate additional currents and fields which can interact with the magnetosphere above and the Earth below. The ionosphere is also the region from which particles can precipitate into the polar regions of the earth and generate aurorae. The conditions produced in the ionosphere induce fields and currents at the surface of the Earth, with a strength that varies depending on the conductivity of the Earth to hundreds of kilometers below the surface. These fields are finally the source of GICs, as long conductors grounded in at least two locations provide a low resistance path for currents to flow. Three graphical depictions of this sequence and the various interactions that take place are shown below.

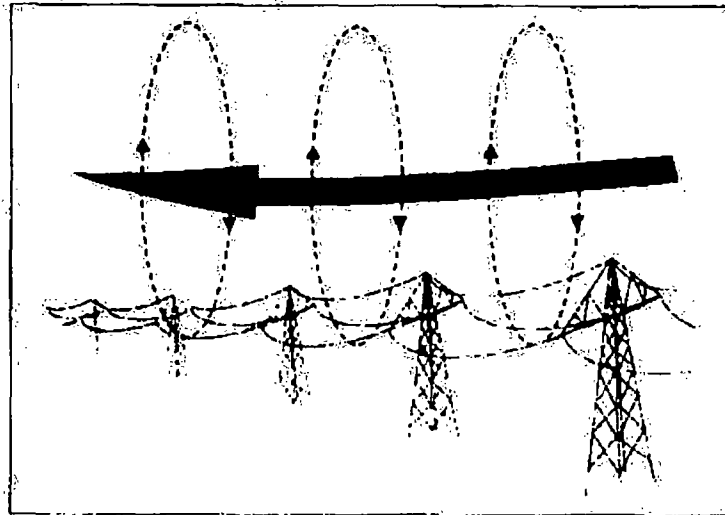


Figure 5: Geomagnetic Induction in Power Systems [7, p. 541]

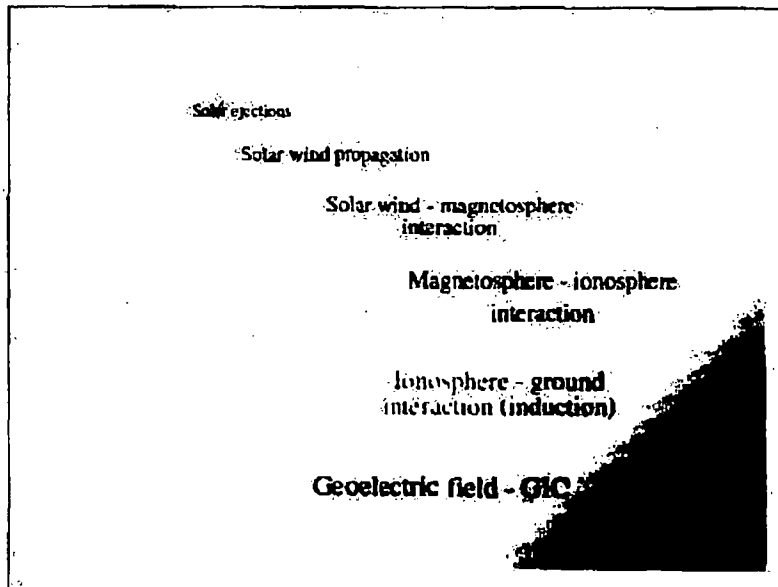


Figure 6: Space Weather Chain of Cause and Effect [8, p. 8]

~~OFFICIAL USE ONLY~~

~~OUO Security Related Information~~

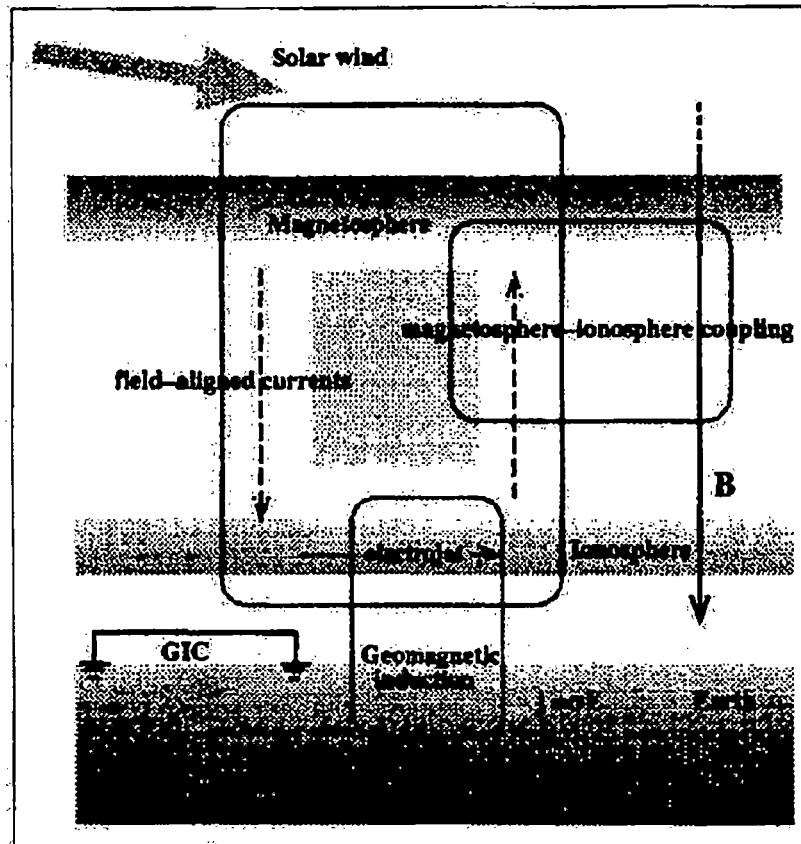


Figure 7: Detailed Diagram of Space Weather Interactions [9, p. 384]

## 2.2.2 Geomagnetic Storms and Substorms

There are still a lot of issues not well understood or agreed upon by the scientific community that monitors, studies and models the Space Weather phenomenon. For example, some use of the term Space Weather as described above, while others use the term to reference all the near-Earth interactions and changes between the interplanetary environment, the magnetosphere and the ionosphere. One of the few points that do seem fairly well established is that there are also two basic types of geomagnetic events that regularly occur and have the potential to produce noticeable effects on the surface of the Earth; these are called geomagnetic storms and substorms.

### 2.2.2.1 Geomagnetic Storms

Geomagnetic storms are caused by the more sporadic events, such as when the plasma cloud from a CME or when a Corotating Interaction Region (CIR) reaches the Earth. A CIR is formed when a faster moving section of the solar wind catches up to a slower moving portion of the solar wind and leading edge and trailing edge shock waves are generated as they interact. This usually happens at distances greater than the Earth's orbit, but it does occasionally happen close enough to the sun that there is a chance the Earth will experience this event.

Geomagnetic storms also generate shock waves when they interact with the magnetosphere and generally have enough energy to compress or reduce the size of the magnetosphere on the sunward side of the Earth, causing increased plasma densities, temperatures and pressures in this region. The magnetosphere reacts to these changes by trying to redistribute the energy around the Earth and down into other regions or zones of Earth's atmosphere. This reaction can induce large voltage potentials at the surface of the Earth and, depending on the conductivity in the region, very large currents as well; see Figure 7. Assuming that the changes in the magnetic fields of the ionosphere can be determined, the electric fields induced at the surface can be found from Equation 2 [10, p. 4-5].

$$E(t) = -\frac{1}{\sqrt{\mu_0 \epsilon}} \int_0^t \frac{\partial B(t-t')}{\partial t'} e^{\sigma t' / 2\epsilon} J_0\left(\frac{1\sigma t'}{2\epsilon}\right) dt' \quad (2)$$

Assuming that  $\epsilon/\sigma$  is very small in comparison to time constants related to geomagnetic phenomenon, the Bessel function can be replaced with its asymptotic large-argument expression to get the following.

$$E(t) = -\frac{1}{\sqrt{\pi \sigma \mu_0}} \int_0^t \frac{1}{\sqrt{t'}} \frac{\partial B(t-t')}{\partial t'} dt' \quad (3)$$

This equation is very similar to equation (1), essentially differing only in a change of variables and the related change in the lower limit of integration. In a similar response to the complexity of modeling and analyzing the complex waveform of the HEMP E3 induced currents, the GIC waveforms are also often described as "quasi-DC" signals and analysis and vulnerability studies are frequently performed using a DC current on the order of ~100A. The similarities between the HEMP E3 electric fields and the electric fields that induce a GIC can clearly be seen in the figure below.

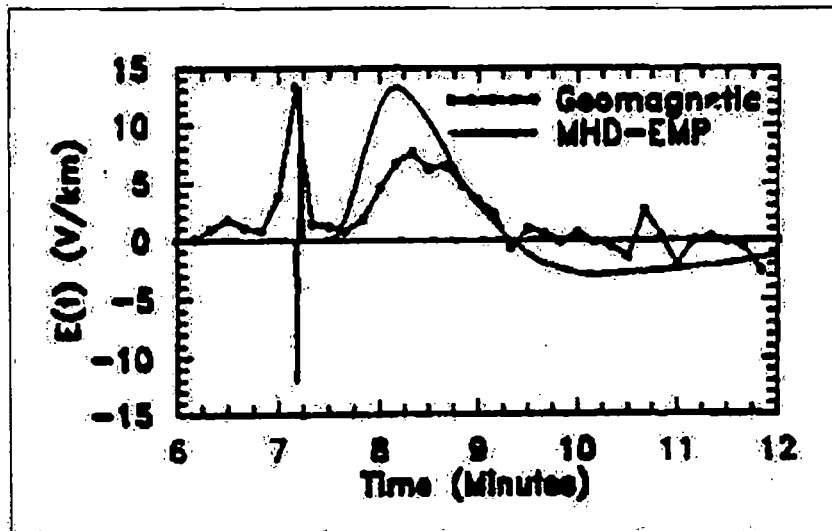


Figure 8: Comparison of MHD and GIC Waveforms [4, p. 15]

Some of the fields that generate GICs are distributed primarily in a geomagnetically referenced, east-to-west directed ring shaped area around the polar regions of the earth. They can be measured as a change in the Earth's undisturbed magnetic field strength of approximately 30,000 nanoTeslas (nT). The issue of where the maximum field values lie is primarily a function of the intensity of the solar wind, the magnitude of the plasma energy coupled into the ionosphere, and the time of year. The area or auroral zone also changes and evolves over a period of hours or sometimes days as the various space weather mechanisms continue to inject energy and particles into the magnetosphere and the magnetosphere reacts and compensates for these changes.

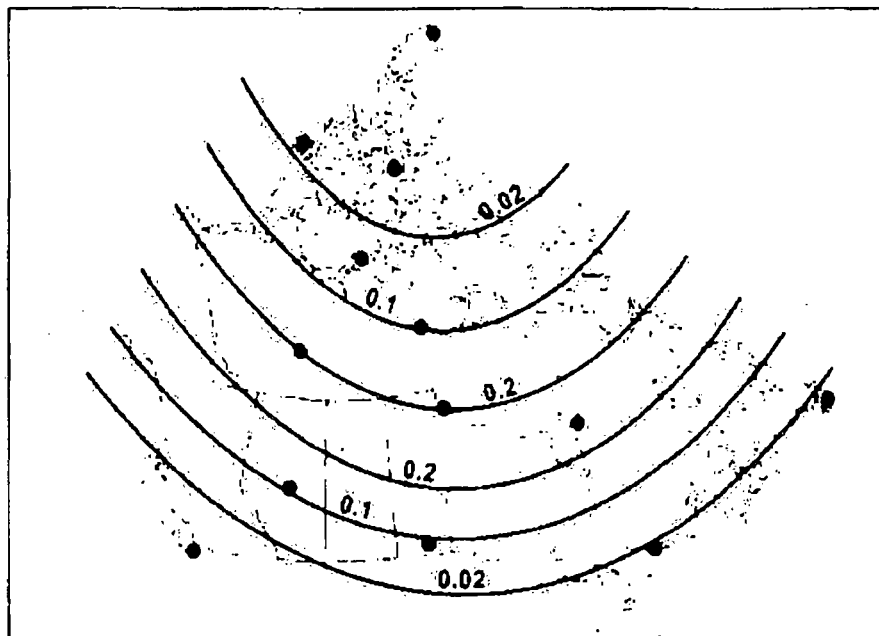


Figure 9: Percent Probability of an Hour with dB/dt in Excess of 300nT/min [7, p. 524]

#### 2.2.2.2 Geomagnetic Substorms

Geomagnetic substorms, on the other hand, occur when the conditions between the "background" solar wind and the magnetosphere interact under specific conditions. Although substorms generally occur more often, if not daily, they usually produce weaker effects at the Earth's surface. Equations (2) and (3) would still be used to find the electric fields induced at the Earth's surface by a substorm, but the expression for the changing magnetic field within the integral would be different. A substorm is specifically created when the magnetic field of the solar wind aligns predominantly northward or southward in relation to the magnetic field of the Earth in the sunward direction, that is, at the point of the magnetosphere where the solar wind first comes into contact with it.

If the solar wind's magnetic field is aligned predominantly northward, the field lines will wrap around the magnetosphere and reconnect with the magnetosphere's field lines just past the poles (anti-sunward) at high northern and southern latitudes, see Figure 10. The fact that the reconnection process occurs is widely accepted, even if the specific physics of this phenomenon are still under debate. The reconnection allows some of the solar wind plasma to couple into the sunward side of the

~~OUO-Security Related Information~~  
~~OFFICIAL USE ONLY~~

magnetosphere, gaining energy as the magnetic field lines shorten and relax into shape. As the overall magnetosphere reacts to this input of magnetic field lines and energetic plasma, field aligned currents flow into and out from the polar regions into the magnetosphere's tail and the Earth's equatorial Ring Current increases. All of these effects can generate fields and voltages at the surface that could potentially induce GICs. This situation, however, is really more of a lesser substorm compared to when the solar wind is aligned predominantly in the southward direction.

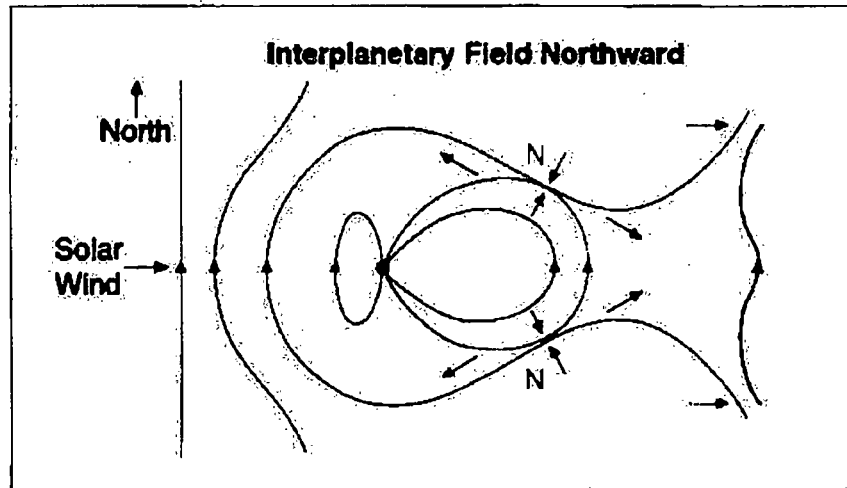


Figure 10: Magnetic Field Reconnection for a Northward Interplanetary Magnetic Field [11, p. 37]

In the case when the solar wind is aligned predominantly in the southward direction, reconnection occurs at the point where the solar wind field lines and the magnetosphere's field lines first meet, at the most sunward point. This creates two open field lines, attached to the northern and southern Polar Regions, which then convect around the Earth to the magnetosphere's tail, where they reconnect with the magnetosphere again, see Figure 11. This process couples a lot more of the solar wind's plasma deep into the tail region of the magnetosphere, where external solar wind pressures and internal reconnection processes can highly energize the plasma. As the reconnection process completes, some of the newly energized plasma is ejected away from the Earth and deeper into the tail as the newly reformed solar wind magnetic field lines continue their interplanetary journey. The rest is injected into lower altitude regions of the nighttime magnetosphere, as newly formed field lines shorten and relax in a manner similar to the dayside field lines of the previous example. As this high energy, high density plasma is added to the nightside magnetosphere, it causes the auroral regions to strengthen and expand towards the equator. This also causes magnetic convection towards the dayside as the magnetosphere tries to return to equilibrium, generating relatively weaker field aligned currents flowing into and out from the Polar Regions into the magnetosphere's tail and relatively stronger increases in the equatorial Ring Current, compared to the northward directed substorm. The more highly variable interaction between the magnetosphere's tail and the solar wind, influencing where and when this second reconnection event occurs, leads to greater extremes in the ionospheric and surface effects produced by the southward directed substorm. Additionally, because of the greater coupling of solar wind plasma, the increased energizing of this plasma by the relaxing magnetic field lines and the non-symmetric nature of a dayside to nightside reconnection pattern versus a near-simultaneous north polar and south polar reconnection pattern, the southward directed substorm-generating solar wind has received substantially more attention in the form of measurements, analysis and modeling than has the northward directed substorm.

~~OFFICIAL USE ONLY~~

~~OUO-Security Related Information~~

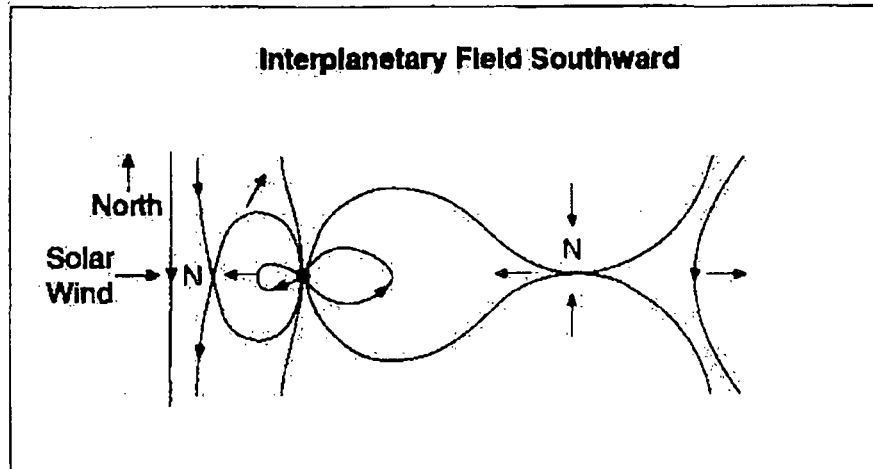


Figure 11: Magnetic Field Reconnection for a Southward Interplanetary Magnetic Field [11, p. 37]

### 2.2.3 Factors Affecting Geomagnetic Events

The likelihood of the solar wind's magnetic field being aligned with the magnetosphere's field is affected by a large number of constantly changing factors. The Earth's magnetic field is not aligned with its axis of rotation. Assuming that the field is similar to that of a magnetic dipole, which is a fairly decent assumption for a simple, first order discussion such as this, the ends of the dipole will be spinning around the Earth's axis. The Earth's axis is also tilted about 23° with respect to its orbital plane, meaning this rotating dipole will present a different directional aspect of itself towards the sun at different times of the year. This fact is clearly shown in Figure 12.

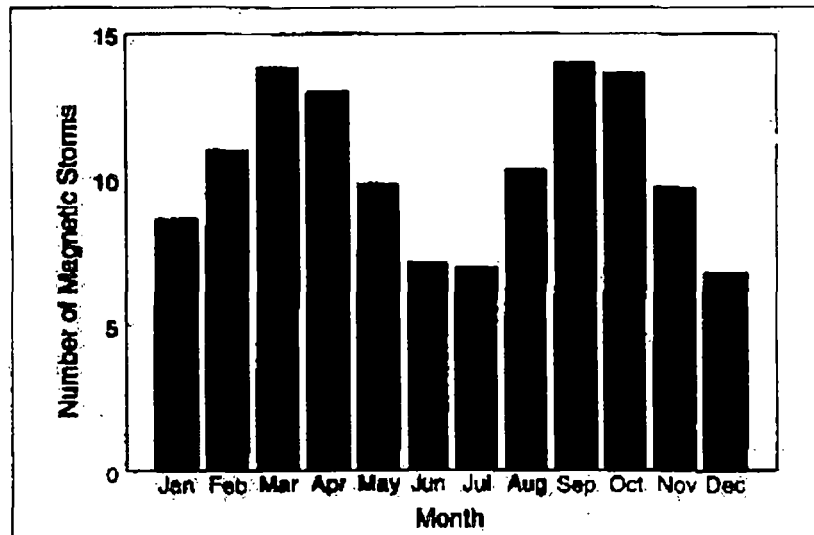


Figure 12: Storm Variations by Month – Averages Based on Data from 1868-1996 [11, p. 544]

The Sun also rotates around an axis that is tilted about  $7^\circ$  from the ecliptic, the plane in which all the planets rotate. The rotational period of the sun varies, from about 25 days at the equator to about 35 days at the poles. Its magnetic field is less like a dipole field than the Earth's, but can still be modeled as a dipole in the simplest discussions, with additional quadrupole terms added if additional accuracy is required. Variation of its rotational speed is suspected of increasing the complexity of the magnetic field-generating processes within the sun, creating an increasing number of sunspots, flares and similar features in a periodic manner. At the end of this eleven-year cycle, the direction of the dipole component of the Sun's magnetic field reverses, and the process begins again, see Figure 13.

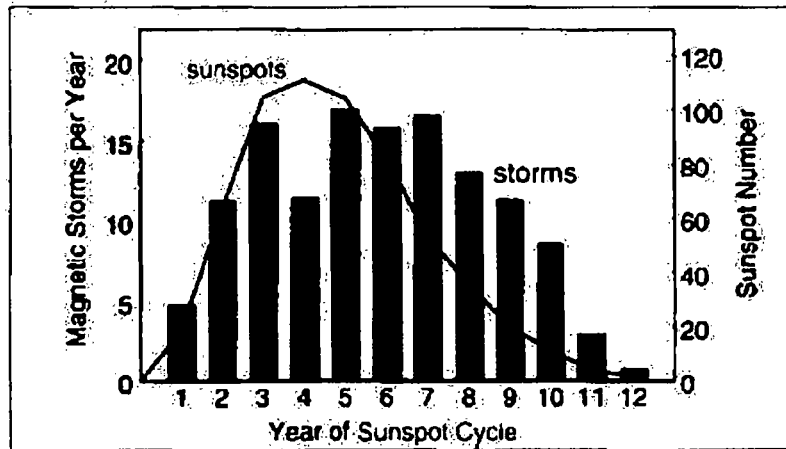


Figure 13: Storm Variations and Sunspot Activity - Averages Based on Data from 1868-1996 [11, p. 543]

The solar wind is primarily generated in regions where local magnetic field structures on the surface of the Sun cause the magnetic field lines to extend outward into interplanetary space rather than curve back around to and close on the Sun in another location. Because the solar wind is comprised of a strongly conducting plasma, the magnetic field lines are "frozen" into the plasma in this orientation, which initially leads to the expectation that all interplanetary field lines should be directed radially from the Sun. However, when the varying rotational speeds and the varying speeds of the solar wind travelling away from the sun are considered, the resulting interplanetary magnetic field lines get curved into a spiral or pinwheel shape, and when the tilt of the sun and the underlying dipole field are considered, the northward and southward components are added to generate a 3D interplanetary field that is described as resembling the twirling skirt of a dancer [12].

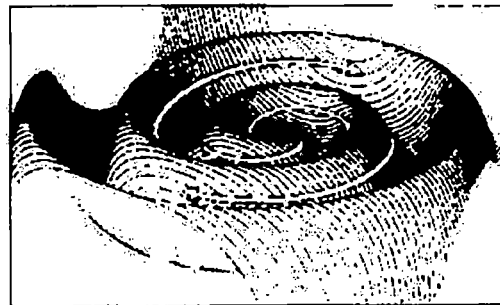


Figure 14: Three-Dimensional Variation of the Interplanetary Magnetic Field [13]

### 3 Analysis Methods and Results

#### 3.1 Coupling Analysis

HEMP E3 and GIC energies produced outside a facility can only interact with the safety systems inside a nuclear power plant if the threat energy can find a means to enter the facility and also be coupled and delivered to the vulnerable components of the systems. As described in detail in the previous report, there are only two realistic methods for signal transmission: 1) for the source field to couple with external elements of the NPP boundary systems, such as above and below ground conduits, power/signal cables, and structural features that can then be conductively carried into the facility's internal structures and components by the internal systems themselves, or 2) for the fields to penetrate the facility directly without a distinct, clearly identifiable conductive mechanism and then couple to corresponding interior elements of the systems. The fact that the field levels in both potential threat mechanisms being reviewed in this report are approximately a million times weaker than the HEMP E1 and HPM fields previously analyzed allows for the second delivery option to be ignored in this report. Thus, the threat calculations performed for this assessment were focused only on the external coupling and transmission scenario. Finally, because coupling to buried cables and pipes is a much more lossy process, and more concerned with issues of corrosion rather than current generation, only overhead line effects will be considered.

The models used to determine the magnitude of the HEMP E3 induced currents coupled into overhead power lines are dependent on a few key variables that all have a specific value at the moment of detonation; the yield of the weapon, the height of the burst, the latitude of ground zero, etc. Obviously, going into greater detail on this potentially sensitive topic is beyond the scope of this unclassified report. Fortunately, most of the work has already been done and documented, as seen in Figure 15 and Figure 16. Note that the maximum current increases with increased line voltage. This is because higher voltage lines usually have lower resistances to reduce loss.

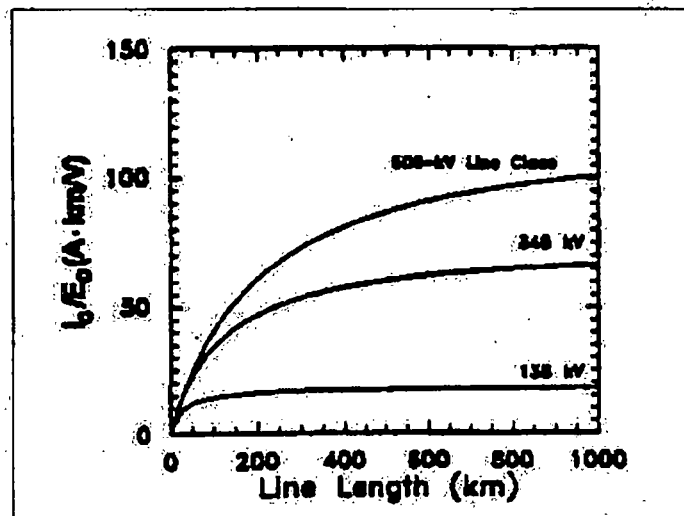


Figure 15: MHD Induced Current Magnitude vs. Length for Three Line Classes [4, p. 25]

~~OUO-Security Related Information~~  
~~OFFICIAL USE ONLY~~

Voltage Class (kV)	$I/E_0$ (A-km/V)
500	120.5
345	74.1
138	18.5
69	16.1
34	13.8
25	13.8
12	11.0

Figure 16: MHD Induced Current Magnitude vs. Line Voltage [4, p.26]

On the other hand, the magnitude of the GICs is dependent on many more variables that are continually changing and dependent on each other in non-linear and poorly understood relationships. This has led to several decades of research and analysis in a constant attempt to develop increasingly accurate models and prediction techniques. Not unlike attempts to model and predict atmospheric weather events, the analysis of space weather and GICs has the benefit of long term statistical databases for model construction and comparison. Data that relates to geomagnetic events has been recorded for over 150 years, albeit when many of the earliest data was collected, its applicability to this field had not yet been recognized. Also, as mentioned earlier, the regular daily occurrence of substorms, most of which are too low in intensity to be of any serious concern, allows for additional data to be constantly collected and for the improvement of models and prediction techniques.

According to Price [14], GIC currents of up to 200A in the neutral line of a three phase power transmission system have been reported in Finland and Sweden, but values of 10 to 15A are more typical in England. Models of the 400kV national power grid in Finland developed by Pirjola [15] predict currents in the range of 50A to 100A per V/km of electric field. Viljanen and Pirjola also state that the largest GIC ever measured in Finland was 201A, for a one minute average, suggesting that the peak was certainly higher. Also, the largest electric field they measured was 4.7 V/km, which led them to state that a 200A to 300A GIC was possible. These values are in the same range as the measurements taken on the power grid in Kazakhstan during seven periods of high geomagnetic activity [16]. In Canada, a model of the 500kV Hydro One power grid also predicts GIC current values in the 25A to 100A per V/km range for north-south oriented electric fields, but also predicts values of 10A to 200A per V/km for east-west oriented fields [17].

It is difficult to definitively compare their relative magnitudes of GIC and MHD induced currents. The MHD induced current magnitude is a function not only of the weapon size and altitude, which determines the size of the MHD's footprint, but also the location of ground zero and the presence, length and orientation of the transmission lines illuminated. Similarly, the GIC's current magnitude is dependent on the relative intensity of the storm, the degree to which the ionospheric currents react and the auroral zone evolves, and the length and orientation of the transmission lines illuminated.

~~OFFICIAL USE ONLY~~

~~OUO-Security Related Information~~

### 3.2 Probability of GIC Occurrence:

Not only has the decades of geomagnetic data collected worldwide been analyzed to predict the possible strengths of GIC induced into the overhead lines of power transmission systems, it has also been studied to help understand the frequency and likelihood of severe storm occurrence. Sensors and recording equipment around the world, and even in outer space, have been put into place over the years to measure and record magnetic and electric field fluctuations. The next two figures are just two of the many statistical results that have been developed using this data. For additional examples and descriptions, more information has been included in Appendix A.

This next figure provides an estimate for the number of times a GIC current can be expected to exceed a given current value for a minimum of 10 seconds in any given year, and even goes so far as to expand this prediction based on whether it is a quiet, average or active year in terms of solar activity. According to this chart, a current of 40A can be expected to occur at least once a year when the sun is quiet, but current of 175A can be expected once a year when the sun is active.

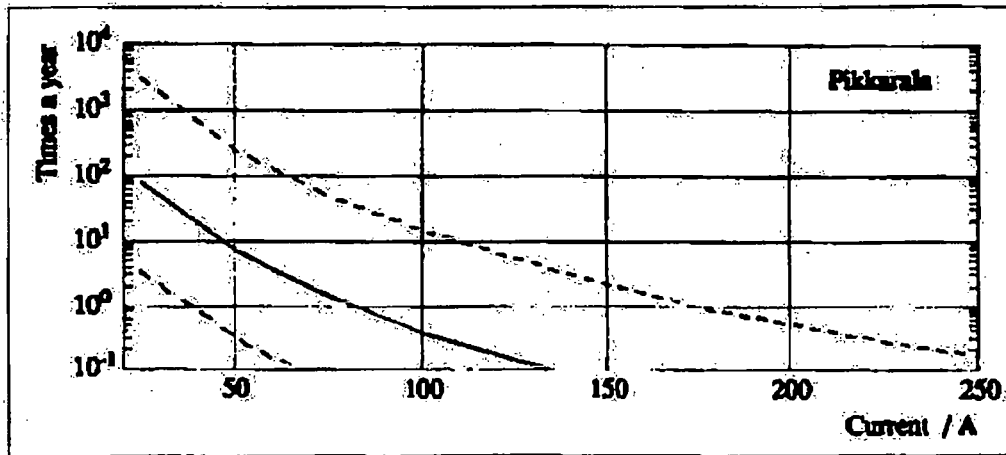


Figure 17: Theoretical Estimates of Annual Number of 10s Currents vs. Amplitude [9, p. 403]  
Note: Lower Dashed Line is for Quiet Years, Upper Dashed Line is for Active Years, and Center Line is for Average Years in Terms of Solar Activity

In a similar analysis, the histogram below (Figure 18) shows the distribution of the lengths of time that over one hundred and seventy of the most severe recorded GIC events lasted. Storm categories and indices are described in more detail in Appendix A, but a severe storm is defined as one that generates surface currents of 100A or more and has a K index of seven or more on a scale from zero to nine. This chart only includes events having currents exceeding 400A and a K Index of 9, and while the great majority of them lasted less than a minute, there have been a few cases where these events have lasted over five minutes.

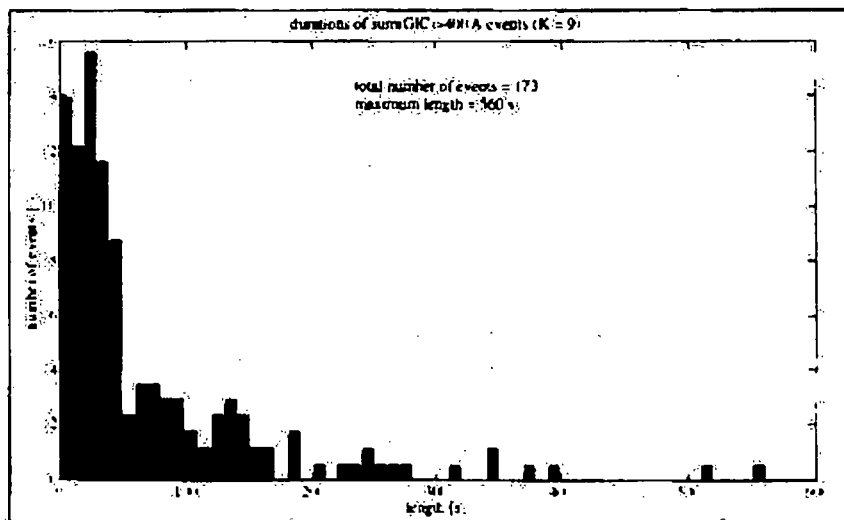


Figure 18: Number of GIC Occurrences vs. Duration in Seconds [8, p. 53]

### 3.3 Analysis of MHD and GIC Effects

Research performed over the last two decades suggests that transformers at the ends or nodes of a transmission line grid absorb the brunt of the damage. The DC nature of the current alters the operating characteristics of the transformer, generating half-cycle rectification effects that manifest as higher order harmonics on the other side of the line. This can lead to an increase in the reactive power demand, tripping compensators designed to protect the overall system [7]. Additionally, the DC currents can saturate the transformer, generating magnetic flux in structural components that were not designed to handle flux and react by heating. Over time, heating of metal parts and other structural components can weaken them and make them more prone to fail. It can also cause bubbles to be generated in transformer oils that sensors can misinterpret as a defect or failure. Saturation of transformers occurs faster when the transformer is operated closer to its maximum load [5]. Often, effects like the generation of harmonics and reactive power demand can change so fast that human monitors of the power grid cannot react fast enough to understand and adjust the system in time to prevent problems, while effects like heat damage can build slowly over long times without any warning until failure occurs.

### 3.4 Potential Consequences of MHD at NPP

While transformers may absorb the brunt of the damage caused by the MHD or GIC signals, they might also pass transients including high frequency harmonics with sufficient strength to be a concern of damage to sensitive electronics. The analysis performed in the previous report [1] determined that the susceptibility levels of NPP instrumentation and monitoring equipment were most often 10A, as determined by various government standards. The magnitude of the currents induced on overhead lines is comparable in magnitude to the currents induced on buried lines by the early time, E1 component of the HEMP generated fields and at least an order of magnitude less than the E1 currents induced in overhead lines. In both cases, as the threat signals propagated through the various electrical networks of cables, buses, transformers and distribution panels, there was sufficient margin to protect the equipment of interest.

#### **4 CONCLUSIONS AND RECOMMENDATIONS**

In addition to recent efforts to consider the vulnerability of sensitive electronic equipment at Nuclear Power Plants to the very short, high intensity threats posed by nuclear HEMP events and conventional High Power Microwave devices, an effort was undertaken to perform a similar analysis of the long duration, low intensity threats posed by HEMP MHD field and Geomagnetic Storm induced currents. Based on decades of research and over 150 years of measurement data, the scientific community has gained sufficient understanding of Geomagnetically Induced Currents to allow for a more statistical analysis rather than the analytic analysis of the earlier effort. Based on this research, it is reasonable to conclude that the magnitude of MHD and GIC currents are approximately the same, with both being sufficiently low in frequency that they can be considered as DC signals for comparison with power transmission systems. Considering all of the variables that affect each current generating mechanism, the MHD and GIC are fairly comparable in magnitude, with their primary difference being that GIC currents are of greater duration. Depending on the time of year and the time of day, as well as the relative level of solar activity, currents of a few amperes can be expected frequently, tens of amperes often and hundreds of amperes occasionally. After a quick comparison with the threat currents and safety margins analyzed and calculated in the previous report, it is considered unlikely that these threats will do any harm to the NPP systems of interest. In fact, the likeliest consequence will be the disconnection of the NPP from the local electrical grid due to transformer failures if not a greater collapse of the transmission line network.

## 5 REFERENCES

1. Wyant, Francis J., et al, "Assessing Vulnerabilities of Present Day Digital Systems to Electromagnetic (EM) Threats at Nuclear Power Plants," SAND Report, December 2009.
2. Ericson, D. M., Jr., et al, "Interaction of Electromagnetic Pulse with Commercial Nuclear Power Plant Systems – Main Report," NUREG/CR-3069, Vol. 2, U.S. Nuclear Regulatory Commission, February 1983.
3. "Electromagnetic Environmental Effects – Requirements for Systems," MIL-STD-464A, 18 March, 1997.
4. Barnes, P. R., et al, "MHD-FMP Analysis and Protection," *DNA-TR-92-101*, Oak Ridge National Laboratories, September 1993.
5. Rabinowitz, Mario, "Nuclear Magnetohydrodynamic EMP, Solar Storms and Substorms," Electric Power Research Institute, Palo Alto, CA.
6. Foster, J. S., Jr., et al, "Report of the Commission to Assess the Threat to the United States from Electromagnetic Pulse (EMP) Attack," Vol. 1, Executive Summary, 2004.
7. Boteler, D. H., "Geomagnetic Hazards to Conducting Networks," *Natural Hazards*, Vol. 28, Kluwer Academic Publishers, 2003, pp. 537-561.
8. Pulkkinen, A., "Geomagnetic Induction During Highly Disturbed Space Weather Conditions: Studies of Ground Effects," *Finnish Meteorological Institute*, No. 24, Academic Dissertation, 1994.
9. Viljanen, A. and R. Pirjola, "Geomagnetic Induced Currents in the Finnish High-Voltage Power System – A Geophysical Review," *Surveys in Geophysics*, Vol. 15, Kluwer Academic Publishers, 1994, pp. 383-408.
10. Pirjola, Risto, "Estimation of the Electric Field on the Earth's Surface During a Geomagnetic Variation," *Geophysica*, Vol. 20, No. 2, 1984, pp. 89-103.
11. Russell, C. T., "The Solar Wind Interaction with the Earth's Magnetosphere: A Tutorial," Dept of Earth and Space Sciences, Institute of Geophysics and Space Physics, University of California, Los Angeles.
12. Daglis, I. A., et al, "Space Storms and Space Weather Hazards," CSP 00-5005, NATO ASI Series, June, 2001.
13. NASA COSMICOPIS Website: <http://helios.gsfc.nasa.gov/solarmag.html>.
14. Price, P. R., "Geomagnetically Induced Current Effects on Transformers," *IEEE Transactions on Power Delivery*, Vol. 17, No. 4, October 2002, pp. 1002-1008.

~~OUO-Security Related Information~~  
~~OFFICIAL USE ONLY~~

15. Pirjola, Risto J., "On the Flow of Geomagnetically Induced Currents in an Electric Power Transmission Network," *Can. J. Phys.*, Vol. 88, 2010, pp 357-363.
16. Vodyannikov, V. V., et al, "Geomagnetically Induced Currents in Power Lines According to Data on Geomagnetic Variations," *Geomagnetism and Aeronomy*, Vol. 46, No. 6, 2006, pp. 809-813.
17. Berge, Jon and R. K. Varma, "A Software Simulator for Geomagnetically Induced Currents in Electrical Power Systems," University of Western Ontario, 2009, pp. 695-700.
18. Barnes, P. R., et al, "Electric Utility Industry Experience with Geomagnetic Disturbances," *ORNL-6665*, Oak Ridge National Laboratories, September 1991.
19. Lakhina, G. S., et al, "An Overview of the Magnetosphere, Substorms and Geomagnetic Storms," Indian Institute of Geomagnetism.
20. Boteler, D. H., "Assessment of Geomagnetic Hazard to Power Systems in Canada," *Natural Hazards*, Vol. 23, Kluwer Academic Publishers, 2001, pp. 101-120.
21. Baker, D. N., et al, "Severe Space Weather Effects – Understanding Societal and Economic Impacts: A Workshop Report," *National Academies Press*, Space Studies Board, 2008.
22. Elias, A. G., and V. M. Silbergleit, "Strong Geomagnetic Disturbances and Induced Currents on Earth Surface," *Progress in Electromagnetics Research Letters*, Vol. 1, 2008, pp. 139-148.

~~OFFICIAL USE ONLY~~

~~OUO-Security Related Information~~

### APPENDIX A: Statistical Data Regarding Geomagnetic Storms

Several different rating systems have developed over the years to measure or describe the intensity of geomagnetic storms. When a storm induces a strong equatorial ring current, flowing from East to West, it will in turn induce a magnetic field that opposes the natural field of the Earth. The change in the magnetic field is measured hourly at four locations near the equator and these four values are averaged to generate a single value called the Disturbance strength, or Dst, in nanoTeslas (nT). The K-index is a quasi-logarithmic scale with its value determined by measurements centered out of Boulder, Colorado. It has a range of 0 to 9 and is based on the maximum horizontal component of the Earth's magnetic field measured over each three-hour period. The Kp-index is basically the same, but is averaged over a network of 14 magnetometers around the globe at locations of 44 degrees to 60 degrees latitude. Because the K and Kp indices are nonlinear, they have been converted to a linear ap index and when eight ap values are averaged, giving a daily value, the result is the Ap index. There is also an Auroral Electrojet (AE) index that averages the readings from seven auroral zone magnetometers 24 times every hour. There are probably as many more indices that haven't been listed here as those that have been. Geomagnetic storms have also been stratified into categories of intensity. Figure 19 is one example comparing two storm indices, their actual magnetic field amplitude ranges and a four-tier category of storm severity levels. For comparison, the undisturbed magnetic field strength of the Earth is approximately 30,000 nT.

Category	A	K	Measured Deviation*
Quiet	0-7	0-2	0-19 nT
Minor storm	30-49	5	70-119 nT
Major storm	50-99	6	120-199 nT
Severe storm	100-400	7-9	200-500+ nT

Figure 19: Comparison of Indices and Associated Magnetic Field Levels [18, p. 4]

According to another category, a magnetic storm is considered to be "Weak" if the Dst index is between 0 and -50nT, it is called "Moderate" if it ranges from -50nT to -100nT, "Intense" when the value falls between -100nT to -500nT, and "Super Intense" when it exceeds -500nT [19]. Clearly, there is no one accepted list of storm categories just as there is no one storm index widely accepted by the geomagnetic community. Several additional figures are shown below that indicate the probability of geomagnetic storms of varying levels of intensity or duration based on various indices described above.

~~OUO-Security Related Information~~  
~~OFFICIAL USE ONLY~~

Figure 20 displays data that suggests storms  $\geq 140$ nT can be expected, on average, once a year while storms  $\geq 300$ nT can be expected, on average, once every ten years. Figure 21 displays data that suggests storms with a Kp index of 5 or more can be expected to occur less than once a month while storms with a Kp index of 8 or more can be expected to occur less than once every year. The data in Figure 20 suggests storms with a Dst  $\leq -200$ nT can be expected to occur 10% of the time in every three week period.

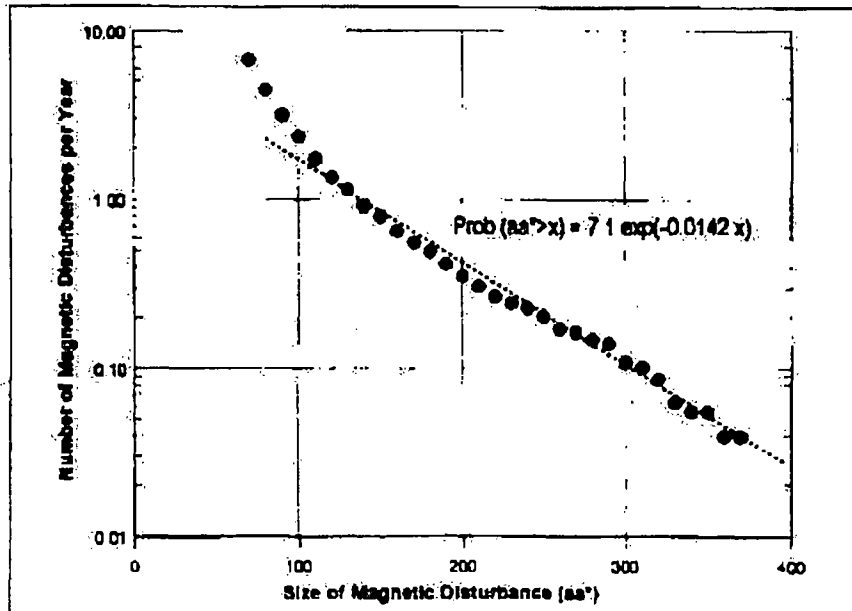


Figure 20: Expected Number of Annual Storms  $\geq 140$ nT vs. Size of Storm (aa) [7, p. 545].

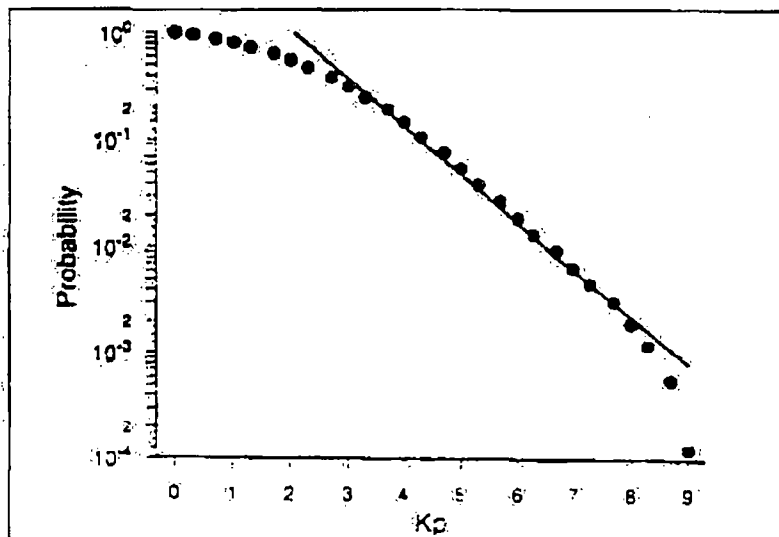


Figure 21: Probability of Annual Storm Occurrence vs. Size of Storm (Kp) [20, p. 114].

~~OFFICIAL USE ONLY~~

~~OUO-Security Related Information~~

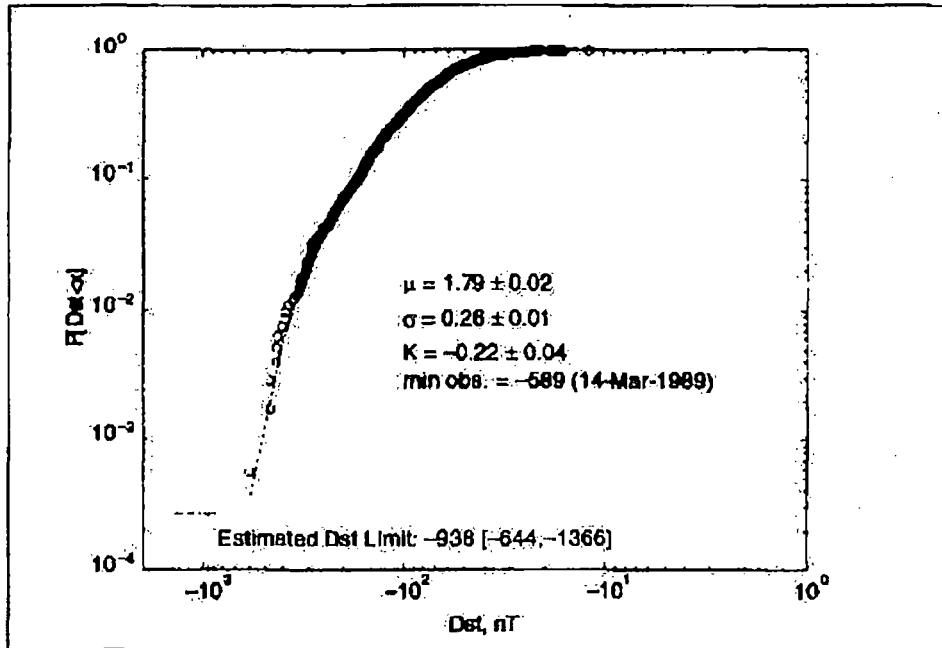


Figure 22: Probability of Storm Size (Dst) in any Twenty Day Period [21, p. 84]

The data plotted in Figure 23, Figure 24, and Figure 25 shows the correlation between various storm indices and the cycle and magnitude of recorded sunspot activity.

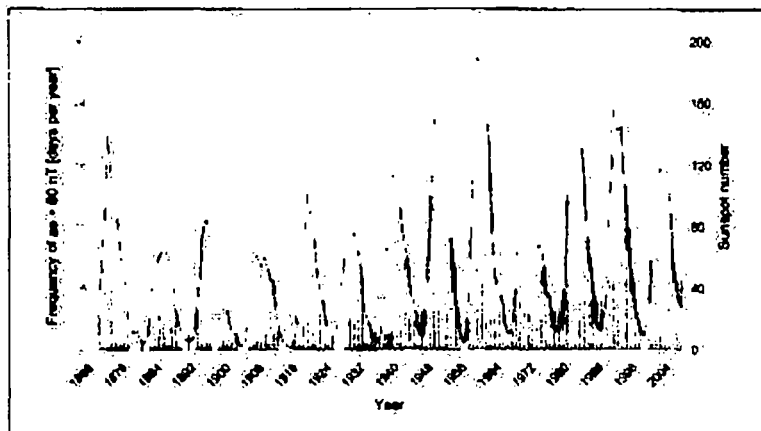


Figure 23: Correlation of  $aa > 80$  nT with Sunspot Activity from 1868-2005 [22, p. 141]

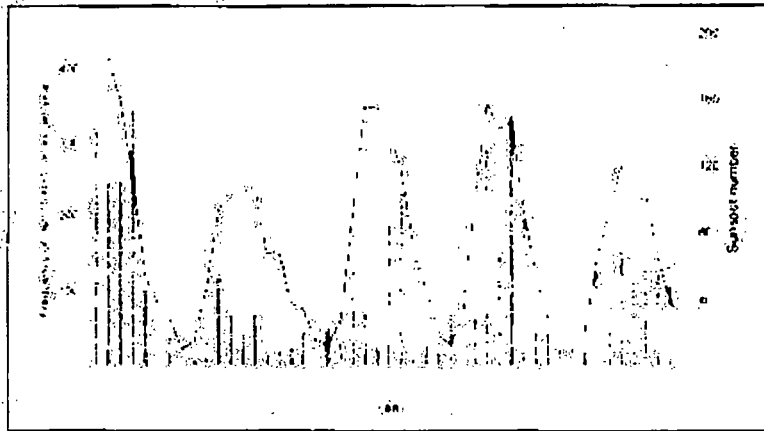


Figure 24: Correlation of Dst < -100nT with Sunspot Activity from 1957-2005 [22, p. 141]

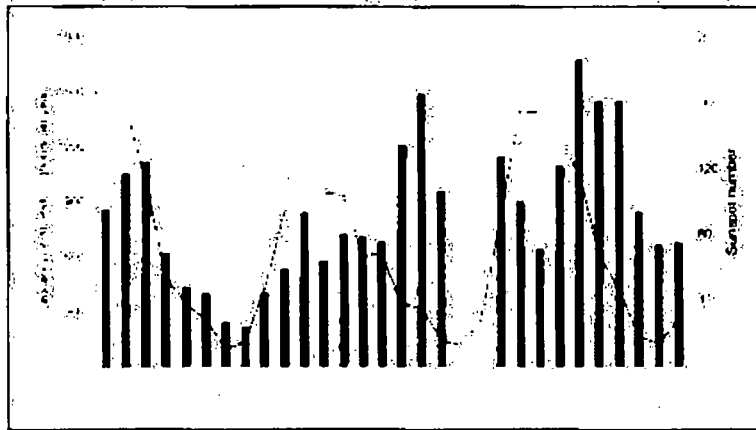


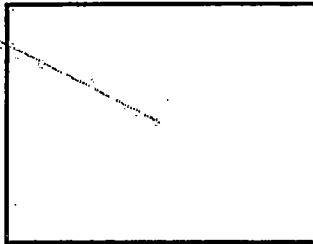
Figure 25: Correlation of AE > 600nT with Sunspot Activity from 1958-2005 [22, p. 141]

~~OUO Security Related Information~~  
~~OFFICIAL USE ONLY~~

**DISTRIBUTION**

R. B. Sydnor USNRC  
L. A. Hardin, Jr. USNRC

(b)(6)



01653  
01653  
05443  
05443  
05443  
06231  
06231

~~OFFICIAL USE ONLY~~

~~OUO Security Related Information~~

~~OUO Security Related Information~~  
~~OFFICIAL USE ONLY~~



~~OFFICIAL USE ONLY~~

25

~~OUO Security Related Information~~